Published by Avanti Publishers

Global Journal of Earth Science and Engineering

ISSN (online): 2409-5710

Stress Regimes and Stress Fields Analysis Using Fault-Slip Data; Eastern Iran

Maryam Ezati[1,*], Ebrahim Gholami[2], Seyed M. Mousavi[2] and Mohsen Ezati[3]

[1]*Department of Civil Enginering, Behbahan Khatam Alanbia University of Technology, Behbahan, Iran*

[2]*Department of Geology, University of Birjand, Birjand 97174-34765, Iran*

[3]*Pasargad Exploration and Production, Tehran, Iran*

ARTICLE INFO

Article Type: Research Article

Academic Editor: Muhamad Yusa

Keywords:
Eastern Iran
Fault-slip data
Stress regime
Sistan suture zone
Stress ellipsoid shape

Timeline:
Received: October 30, 2023
Accepted: December 15, 2023
Published: December 30, 2023

Citation: Ezati M, Gholami E, Mousavi SM, Ezati M. Stress regimes and stress fields analysis using fault-slip data; Eastern Iran. Glob J Earth Sci Eng. 2023; 10: 71-92.

DOI: https://doi.org/10.15377/2409-5710.2023.10.5

ABSTRACT

In this paper direction of stress tensors and stress ellipsoids shape in Neogene, Paleogene, and older units were investigated. Moreover, relationship between shape of stress ellipsoid and exhumation of igneous units were determined using analysis of stress tensors. Analysis of relationships between stress regime and uplifting indicate that in the areas we observed the uplifting of the igneous units the shape of stress ellipsoid has been displaced locally from prolate to oblate which is due to local change of stress regime. Hence, local variation of stress regime in the eastern part of Shekarab Mountains caused boarder outcrops of igneous units. In the western part of study area shape of stress ellipsoid is prolate and it's due to existing reverse fault with strike-slip component. Comparison shape of stress ellipsoid in Eocene units indicate that shape of stress ellipsoid in the western, middle and eastern Shekarab Mountains is prolate, and as local there is oblate stress ellipsoid shape in eastern part. Results of this research indicate that direction of major stress axis had clockwise rotation from Cretaceous times to the present.

*Corresponding Author
Email: Maryamezati.777@gmail.com
Tel: +(98) 9169727149

1. Introduction

Iran is located in the seismic belt of the Himalayan Alps, which extends from west to east from the Mediterranean to Asia. The current tectonics of Iran is caused by the north-south convergence between the Arabia plate to the southwest and Eurasia plate to the northeast [1, 2]. This convergent is accommodated across the Iranian Plateau and adjacent deformed zones, and the deformation, as defined by seismicity and geology is not uniformly distributed. Much of the deformation is concentrated in the Zagros Fold and Thrust Belt in the SW, Alborz Thrust Belt bordering oceanic crust of the south Caspian depression, Kopeh-Dagh Fold Belt in the NE, and in East-Central Iranian thick-skinned range and basin province [3, 4]. The Sistan suture zone, which located in Eastern Iran is the subject of this paper, separates the Lut block and the Afghan block and is characterized by different structural elements and rock associations [4, 5]. Continental collision includes brittle and coeval compressional, extensional and strike-slip faulting in the upper crust [6-8]. Determining stresses allows better understanding the mechanical manner of geological materials and decipher tectonic mechanisms from those associated to plate motion at a large scale to those creating jointing and faulting [9]. Near-surface stress patterns, influenced by topography, control the size and location of the largest landslides [10-12].

Study the reasons of the non-uniform distribution of rock units along the mountains range requires structural analysis of tectonic processes and analysis of stress changes along the mountains range. Meanwhile, the analysis of the steps of applying stresses over the orogeny can provide valuable information about the evolutionary process of the mountainous ranges. Stress pattern of Shekarab Mountains based on brittle structures such as faults have been presented in this paper. This work intends to reconstruct the paleostress regime that is related to the evolution of the Shekarab Mountains structures. We carried out paleostress calculations from fault data within Cretaceous to Quaternary rocks in order to constrain the orientation of the paleostress fields during evolution of Shekarab Mountains. In this research, relationship between shape of stress ellipsoid and exhumation and will be determined using dynamic and geometric analysis of the structures orientation of stress tensor.

The purpose of this study is to investigate the variation of stress pattern (direction of stress tensors and stress ellipsoids shape) in Shekarab Mountains. This research will help us to understand how the main axes of stresses are oriented, the mechanism of the emergence of structures and how they are deformed. Due to the study area is located in Sistan suture zone, by studying the effects and evidence of long-standing tension, it is possible to complete and correct existing information on the development of the Sistan and Collision zones. The orientation and shape of the stress ellipsoid with respect to earth's surface shows the type, orientation and slip sense of faults developed in an area [13]. The state of stress in rocks is generally anisotropic and is defined by stress ellipsoid axes, which characterize the magnitudes of the principal stresses. In positive compression, the longest axis is the ellipsoid's major stress (σ1), the intermediate axis is the intermediate stress (σ2), and the shortest axis is the minimum stress (σ3). Stress inversions from fault slip measurements have now become a common tool in tectonics. They are used for characterizing ancient stress fields, and also in active tectonics [10, 13, 14]. The study area (Shekarab Mauntains) is created by a terminal splay of the Nehbandan fault located in the Sistan suture zone (Fig. **1**). Litology map of the study area shows that study area is composed of Peridotite (upper Cretaceous), phyllite (upper Cretaceous), flysch (upper Cretaceous-Paleocene), tuff (middle Eocene), andesite (upper Eocene-Oligocene), dacite (Neogene) (Fig. **2**). So far, no attempt has been made to study the relationship between shape of stress ellipsoid and exhumation in Shekarab Mountain. In this research, relationship between shape of stress ellipsoid and exhumation and will be determined using dynamic and geometric analysis of the structures orientation of stress tensor.

Inversion computes a mean best fitting deviatoric stress tensor from a set of at least four striated faults by minimizing the angular deviation between a predicted slip vector (maximum shear) and the observed striation [13, 15, 16]. This method assumes that rigid block displacements are independent and have been used in various regions: eastern Turkey and the Caucasus [17], Denizli Basin (Western Turkey) [18], Oslo region [19], Sikkim Himalayan [20], NE Iran [21], central Kopeh dagh [22], Lusatian Fault Belt [23], NW Pakistan [24], Caddapah basin, India [25], western Ordos fold-thrust belt, China [26], Shimanto accretionary complex [27], northern Eastern Ghats Province, India [28], Suture Zone Sistan, Iran [29], Eastern Iran [30], Shekarab Mountain, Iran [31], Eastern Iran [32], Northern Birjand, Eastern Iran [33], central Apennines, Italy [34], eastern Mediterranean [35], Yanbian area NE

China [36], Central Andes Bend [37], Pioneer metamorphic core complex, Idaho [38], East Iran Orogen [39], Southern Alps [40], South China [41].

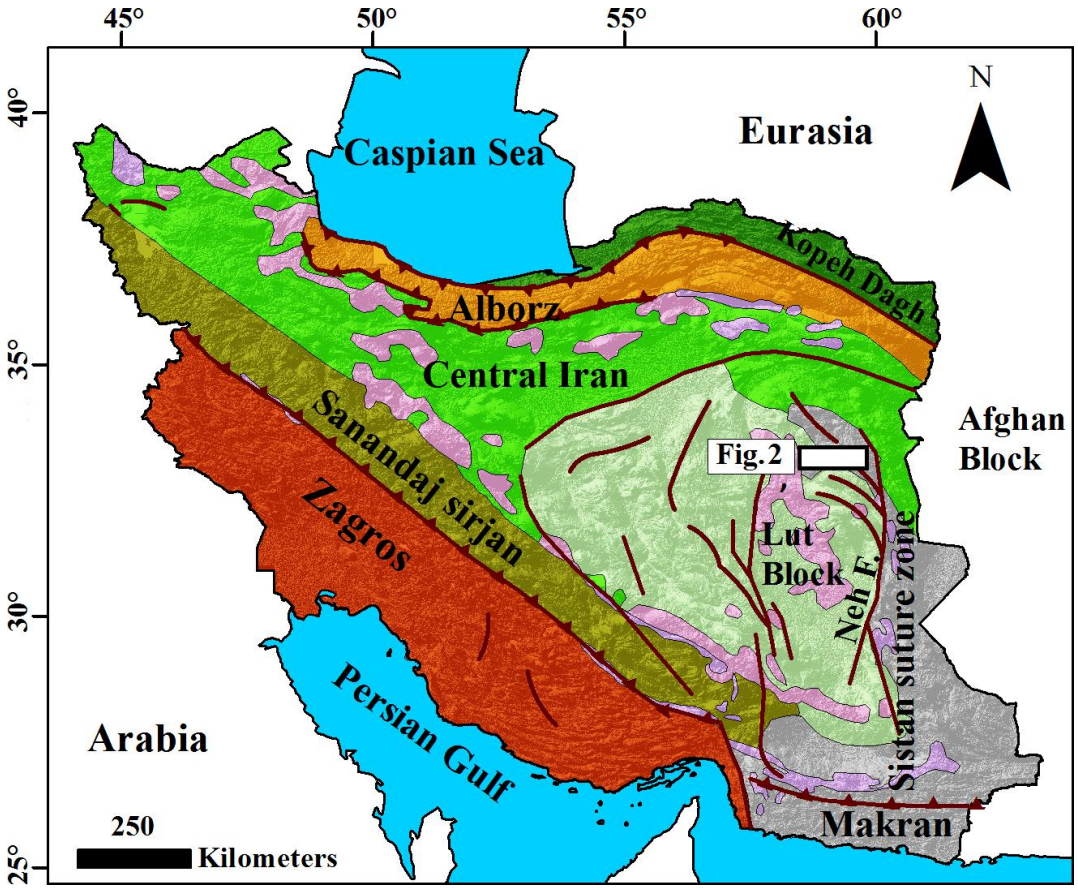

Figure 1: The Structural-Sedimentary zones of Iran, Neh. F = Nehbandan Fault. Location map of the study area is indicated by white rectangular.

2. Tectonic and Geological Setting

To study the evolution of the Sistan Ocean several investigations can be done on N-S, E-W and NW-SE trends. With Investigating of the relationship between shape of stress ellipsoid and exhumation we can discover the evolution of Shekarab Mountain in the E-W tread. This study will indicate some aspects of tectonic Evolution of the Sistan mountain range and other collisional areas. Shekarab Mountains is located in eastern Iran, longitudes and latitudes of the study area are 58˚37E to 59˚16E and 32˚50N to 33˚09N, respectively (Fig. **1**). Lithology map of study area indicate that study area is composed of Peridotite (upper Cretaceous), phyllite (upper Cretaceous), flysh (upper Cretaceous-Paleocene), tuff (middle Eocene), andesite and dacite (upper Eocene-Oligocene). Shekarab Mountains is created by a terminal splay of Nehbandan fault that is located in the Sistan suture zone (Fig. **2**). Sistan structural zone is a north-south trend and represents the suture between Lut block and Afghan block [5]. The Sistan suture zone is dominated by major N-S or NNW-SSE right-lateral strike-slip faulting with some NW-SE reverse faults and some E-W left-lateral strike-slip faults [42, 43]. The existence of Nehbandan fault system in the border between Sistan suture zone and Lut block has caused several rock units in the margins and within the structural state of Sistan. Nehbandan fault system with strike-slip mechanism by north-south general trend has sub-branches in the North and South terminals. Northern terminal of Nehbandan fault has rotated toward west and its southern terminal toward east [44]. So far, there has been no attempt to study relationship between the changes of stress ellipsoids shape along the mountains. Therefore, the results of this study can be an effective step in solving structural complexities along the mountains. The results of this research will provide a new insight into the history of tectonic evolution in the E-W trend of Mountain ranges.

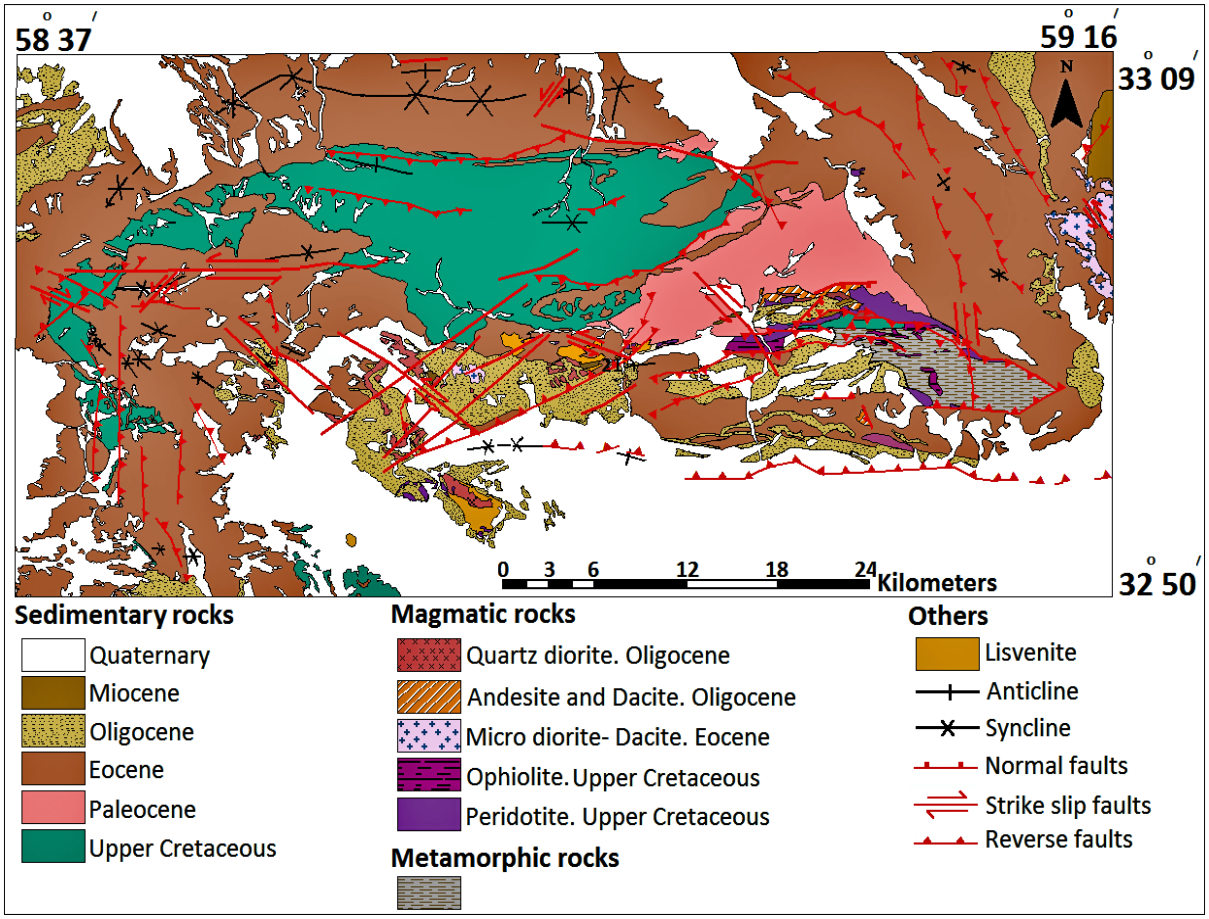

Figure 2: Geological map of the Shekarab Mountain was modified from [45].

3. Material and Methods

We adopted the direct stress tensor inversion method [13, 46] for computation of the state of paleostress. Stress tensor inversion method is based on maximizing the sum of slip shear stress in the direction of actual slip for the entire data set. This sum is calculated as a function of four independent variables of the reduced stress tensor, i.e. three angular parameters for orientation of the principal stress axes of stress σ1≥ σ2 ≥ σ3, as well as the ratio of the principal stress magnitude differences calculated as Φ =(σ2-σ3)/(σ1-σ3), given the orientation and shape of stress ellipsoid [13, 47]. Inversion results include the azimuth and plunge of the principal stress axes (σ1, σ2, and σ3) as well as a stress ellipsoid shape parameter Φ ratio (Φ = (σ2-σ3)/(σ1-σ3)≤1). Principal stress axes σ1, σ2, and σ3 correspond to the compression, intermediate and extension, respectively. Stress regime can be determined with both of orientation stress axes and Φ ratio: a) when σ3 is vertical, the stress regime is purely compressional, when Φ ratio is close to 0.5 (between 0.75 and 0.25, σ1> σ2> σ3), radial compressional when Φ ratio is close to 1 (between 0.75 and 1 σ1≈ σ2), and transpressive when Φ ratio is close to 0 (between 0.25 and 0, σ2≈ σ3), b) when σ1 is vertical, the stress regime is purely extensional when Φ ratio is close to 0. 5, radial extensional when Φ ratio is close to 0 and transtensive when Φ ratio is close to 1; c) when σ2 is vertical, the stress regime is purely strike-slip when Φ ratio is close to 0.5, transtensive when Φ ratio is close to 1, and transpressive when Φ ratio is close to 0 [13, 15].

The general stress tensor (first matrix term (**T**)) is associated with the stress tensor in the principal stress coordinate system as follows:

$$\begin{pmatrix} a & d & f \\ d & b & e \\ f & e & c \end{pmatrix} = \begin{pmatrix} x1 & x2 & x3 \\ y1 & y2 & y3 \\ z1 & z2 & z3 \end{pmatrix} . \begin{pmatrix} \sigma1 & 0 & 0 \\ 0 & \sigma2 & 0 \\ 0 & 0 & \sigma3 \end{pmatrix} . \begin{pmatrix} x1 & y1 & z1 \\ x2 & y2 & z2 \\ x3 & y3 & z3 \end{pmatrix} \quad (1)$$

This is the matrix expression of a tensor rotation: the transfer from the system of principal axes into a general system of Cartesian coordinates. The expressions

$$\begin{pmatrix} x1 \\ y1 \\ z1 \end{pmatrix}, \begin{pmatrix} x2 \\ y2 \\ z2 \end{pmatrix}, and \begin{pmatrix} x3 \\ y3 \\ z3 \end{pmatrix}$$

are the unit vectors along σ1, σ2, and σ3. The stress vector σ acting on a fault plane characterized by its normal unit vector **n** is given (Fig. **2**), in vector and matrix notations successively, by the following equations:

$$\sigma = \mathbf{Tn} \tag{2}$$

$$\begin{pmatrix} \sigma x \\ \sigma y \\ \sigma z \end{pmatrix}, \begin{pmatrix} a & d & f \\ d & b & e \\ f & e & c \end{pmatrix} . \begin{pmatrix} x \\ y \\ z \end{pmatrix} \tag{3}$$

The modulus of the normal stress (ν) is given by the scalar result of the stress vector using the normal unit vector by the following equations:

$$|\nu| = \sigma . n \tag{4}$$

$$\text{Order } |\nu| = x\sigma_x + y\sigma_y + z\sigma_z \tag{5}$$

The normal stress vector (ν) is then:

$$\nu = |\nu| n \tag{6}$$

$$\begin{pmatrix} \nu_x \\ \nu_y \\ \nu_z \end{pmatrix} = |\nu| \begin{pmatrix} x \\ y \\ z \end{pmatrix} \tag{7}$$

Recognizing the stress vector (σ), the normal stress vector (ν) and the shear stress vector (τ) is

σ = ν + τ that is:

$$\begin{pmatrix} \tau_x \\ \tau_y \\ \tau_z \end{pmatrix} = \begin{pmatrix} \sigma_x \\ \sigma_y \\ \sigma_z \end{pmatrix} - \begin{pmatrix} \nu_x \\ \nu_y \\ \nu_z \end{pmatrix} \tag{8}$$

Reduced stress tensor: by adding to the stress tensor isotropic stress defined by $| = -\sigma_3$, then multiplying the tensor by the positive constant k = 1/(σ1 − σ3), one obtains

$$\begin{pmatrix} \sigma1 & 0 & 0 \\ 0 & \sigma2 & 0 \\ 0 & 0 & \sigma3 \end{pmatrix} \rightarrow \begin{pmatrix} 1 & 0 & 0 \\ 0 & \Phi & 0 \\ 0 & 0 & 0 \end{pmatrix},$$

both tensors are equivalent in terms of directions and senses of shear stresses (remember Φ = (σ2-σ3)/ (σ1-σ3)). The resulting "reduced stress tensor" contains four independent variables, and simply depends on the orientation of the principal stress axes and the ratio Φ

$$\begin{pmatrix} x1 & x2 & x3 \\ y1 & y2 & y3 \\ z1 & z2 & z3 \end{pmatrix} . \begin{pmatrix} 1 & 0 & 0 \\ 0 & \Phi & 0 \\ 0 & 0 & 0 \end{pmatrix} . \begin{pmatrix} x1 & y1 & z1 \\ x2 & y2 & z2 \\ x3 & y3 & z3 \end{pmatrix} \tag{9}$$

The variables k and | cannot be determined from fault-slip orientations and senses. Whereas the reduced stress tensor has four autonomous variables; therefore, at least four distinct fault-slip data are needed to calculate it [13].

In this research, the right dihedra, direct inversion and ratio of stress magnitude difference methods by Win-Tensor software were used to obtain orientation and shape of the stress ellipsoid. The Win-Tensor data base contains site description data, orientation data for geological brittle structures, subset description and solutions

recording. Both PBT and Right Dihedron methods allow a direct estimation of the stress axes orientation and relative magnitude. PBT is based on the average orientation of areas of p, b, c kinematic axes of all individual data. Right Dihedron is based on areas of compression and extension associated to right dihedrons of all individual data combined in a single stereonet and representing the possible orientation of s1 and s3 stress axes. These two methods produce approximate results that are refined with the Rotational Optimization procedure [48].

4. Discussion

In this research, for obtaining stress tensor inversion, brittle structures, including the orientation of fault surfaces, slickenside lineation, and sense of motion indicators, have been collected. For determining stress tensor orientation and stress field in different geological age, we separated the data sets into homogeneous subsets in order to reconstruct various stress fields in the study area. We separate brittle structures related to different geological age, the state of stress, and stress tensor orientation calculated utlizing Win-Tensor software. The main objectives of this research are: recognition and comparison of the stress ellipsoids shape in Neogene units (around the mountain units), Paleogene (in the igneous units) and if possible older units; analysis of relationships between stress changes and exhumation in the East-West trend mountain range; understanding the variations of the stress ellipsoids shape along the mountain range; analyzing the tectonic pattern of the study area and its evolution during geological times. Multiple direction slickensides were not occurred in a single phase of deformation, but they have been created as a result of several phase of deformation. Existing several slikenlines on a single fault plane is due to changes of stress over time. We mean that the primary stress regime was compressional which causes the faults with strike-slip, compression, and tension components in the study area. R: is stress ratio; Right Dihedron method has given only an estimate of orientations of the σ1, σ2, and σ3 axes. The moment stress axes P, B, and T axes demonstrate the maximum shortening, the unbiased axis, and the maximum extension, respectively. These faults occurred on rock unites; hence, they are post tectonic. No research has been related to the syn-tectonic faulting. Some of the faults in the Shekarab Mountains only cut the units related to certain times, such as F21 and F22 faults cut the Cretaceous units. Therefore, these faults are belong to the the Cretaceous time stress regime and have not been reactivated by younger tectonic regimes. However, the F5 and F14 faults that cut the Paleocene, Eocene, Oligocene, Neogene, and Quaternary units have been reactivated by younger tectonic regimes. The outcrops of peridotite, andesite and dacite are prevalent in the eastern part of Shekarab Mountain. To find its reason, the brittle structures model was considered to reconstruction the Paleostress regime changes. So far no any study has been carried out on relationship of stress regime changes and exhumation in Sistan suture zone. Hence, this research can increase field and theoretical knowledge on the structural complexities in this mountain range. Also, this research will help to find the answers of the questions: how does the stress regime changes in the mountain ranges where the dispersion of lithology is heterogeneous? What caused the heterogenic distribution of rock units in the mountain range? Why ophiolites are more evident in the eastern part of study area? In order to obtain the direction of stress axes in each geological period, first fault data related to all different times were collected and the following were done:

1. To obtain the direction of stress axes in the Quaternary, the faults related to the Quaternary time were separated from all data set and by using these faults the stress tensor in the Quaternary time were determined.
2. In order to obtain the direction of stress axes in the Pliocene time, the fault data collected in the units related to the Pliocene were separated from the primary faults, then in the data related to the Pliocene, we removed the faults which have similar geometric-kinematic position (trends of the faults and rakes of the slickenlines) to the Quaternary faults and Using the remaining faults, the stress axes related to the Pliocene time was obtained.
3. For calculating the stress axes direction in the Miocene time the fault data collected in the Miocene units were separated from the primary faults, then the faults which have similar geometric-kinematic position (trends of the faults and rakes of the slickenlines) to the Pliocene and Quaternary faults were removed from the Miocene fault data. Moreover, using the remaining faults the stress axes related to the Miocene time were obtained.

4. To obtain the stress axes direction in the Oligocene: the fault data that was collected in the Oligocene units was separated from the primary faults, then we removed the faults whose geometric-kinematic position were similar to the Pliocene, Miocene, and Quaternary faults and by using the rest of the faults, we obtained the stress axes of the Oligocene time.
5. To obtain the stress axes direction in the Eocene: the fault data collected in the Eocene units were separated from the primary fault data set; moreover, in the Eocene fault data which have similar to the Oligocene, Pliocene, Miocene, and Quaternary faults Were removed and using the remaining faults the stress axes related to the Eocene time was obtained.
6. To obtain the stress axes direction in the Paleocene: the fault data collected in the Paleocene units were separated from the primary fault data set, then in the Paleocene data the faults which have similar geometric-kinematic position to the Eocene, Oligocene, Pliocene faults, Miocene, and Quaternary, were removed and using the remaining faults the trends of stress axes related to the Paleocene were obtained.
7. To calculate the directions of stress axes in the Cretaceous: we removed the faults which have similar geometric-kinematic position to the Paleocene, Eocene, Oligocene, Pliocene, Miocene and Quaternary faults in the fault data have been collected in the Cretaceous units. Moreover, using the remaining faults which their trends were not similar to any of the faults related to the previous times the trends of stress axes related to the Cretaceous time were obtained.

Faults are one of the most important structures in the Shekarab Mountains. In this research fault slip data including spatial orientation of fault planes and associated striae were collected across Shekarab Mountains, the data set collected from study area were processed using Right Dihedron, PBT axes, and Rotational Optimization methods. Paleostress analyses were used for determining steps of applied stress over the Shekarab mountains range. In this research after collecting data from field operations we prepared Structural map, the study area were divided in to three parts: Eastern, middle and western based on mechanism and strike of the faults, to obtain stress regime and orientation of the principal stress axes. Geometric and kinematic analysis of identified faults indicate that mechanism of most study areas faults are reverse with dextral strike-slip component and strike-slip with reverse component which indicated the overcoming of compressional stress in Shekarab Mountains. In this research to obtain the orientation of the principal stress axes brittle structures such as faults were investigated. In Structural map of Shekarab Mountains several pictures of study areas faults that have been taken from field operations are indicated (Fig. **3**, **4**). The Mohr circles were plotted using the values of the three principal stresses

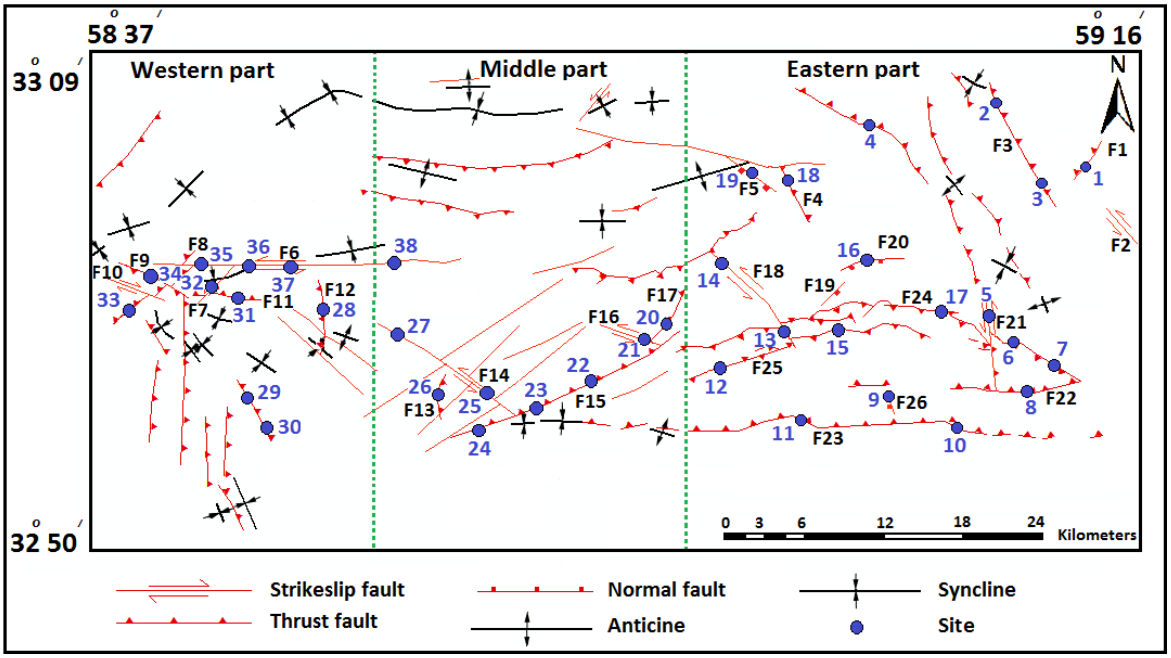

Figure 3: Structural map of the studied brittle structures (faults) in field operations.

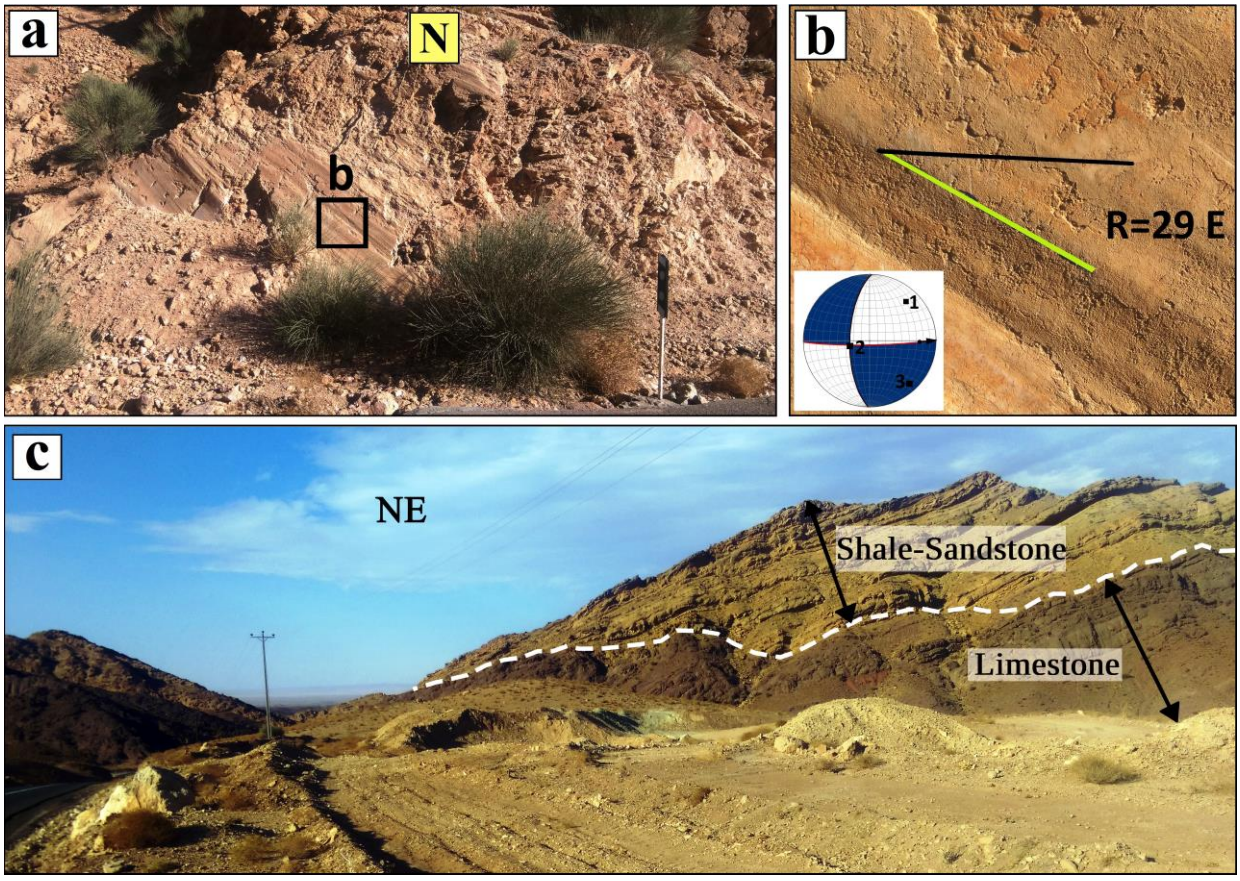

Figure 4: a) Field photo of a Sinistral strike-slip fault with N087˚, 83S geometric position; **b**) slickenline on the minor fault. In the stereonet, numbers 1, 2, and 3 indicates orientation of the principal stress axes; **c**) Moderate dipping strata (~35˚) in the southern limb of the great syncline are demonstrated in the B-B' profile.

σ1, σ2, and σ3. The largest Mohr circle is defined by the difference between σ1 and σ3, and the two smaller Mohr circles are defined by the differences between σ1 and σ2, and σ2 and σ3, respectively. In a normal stress regime, the size of the Mohr circle is controlled by the difference between σV (as σ1) and σhmin (as σ3) (i.e., σ1- σ3). In a strike-slip stress regime, the size of the Mohr circle is controlled by the difference between the two horizontal stresses (σHmax-σhmin), and the circle will shift to the right equally, which means it will not change in size (Fig. **5**).

In this paper Shekarab Mountains divided in to Eastern, middle and western parts. In the eastern part of Shekarab Mountains most of the faults mechanisms are reverse and they have East-West strike, which locally there is normal faults. In the middle part faults have strike-slip mechanism and North East-South West strike. In the western part of study area most of the faults have reverse mechanisms and North-South strike. The objective of this paper is to investigating the variations of stress tensor's direction and stress ellipsoids shape from Cretaceous units to younger units. Igneous units have been more outcrops in eastern part than other part of study area, for determining the reason of non-uniform distribution of rock units along the Shekarab Mountains the step of applied stress over the study area were analyzed and provide valuable information about the evolutionary process of the Shekarab Mountains. We attempt to make a relationship between stress field changes and exhumation of igneous using orientation of stress tensors; therefore, in three part of study area (Eastern, middle, and western) Stress regime changes from Cretaceous units to Quaternary units were determining. The outcrops of Cretaceous and Paleocene units are in eastern part of the study area, most of Cretaceous units in the Shekarab Mountains are Peridotite. In Cretaceous units major stress axis (σ1) had NW-SE trend and stress regime operation was strike-slip (Fig. **5**). In Paleocene units major stress axis (σ1) had W-E trend and stress regime operation was strike-slip (Fig. **6**). Eocene units are exposed in three parts of the study area, in the rock units of Eocene major stress axis (σ1) had North-South trend and stress regime operation was transpressive (Fig. **7**-**9**). Most outcrops of igneous units (andesite and dacite) by the age of Eocene are related to the eastern part of the

Shekarab Mountains. In the sections of the Shekarab Mountains we observed the uplift of igneous units orientation of σ1 is vertical, the Φ ratio is close to 0.5, stress regime is purely extensional and the shape of stress ellipsoid has been displaced locally from prolate to oblate which is due to local changes in the stress regime (Fig. **10**). In the eastern and middle part of Shekarab Mountains there are Oligocene units, stress component of Oligocene rocks in study area have NE-SW trend and stress regime is strike- slip (Fig. **11**, **12**). Paleostress analyses in Miocene rocks indicate that in the Miocene geological time stress components had NE-SW trend and stress regime was strike-slip (Fig. **13**). The Quaternary rocks exist only in the middle part of the study area, stress component in Quaternary rocks has NE-SW trend and stress regime is strike-slip (Fig. **14**).

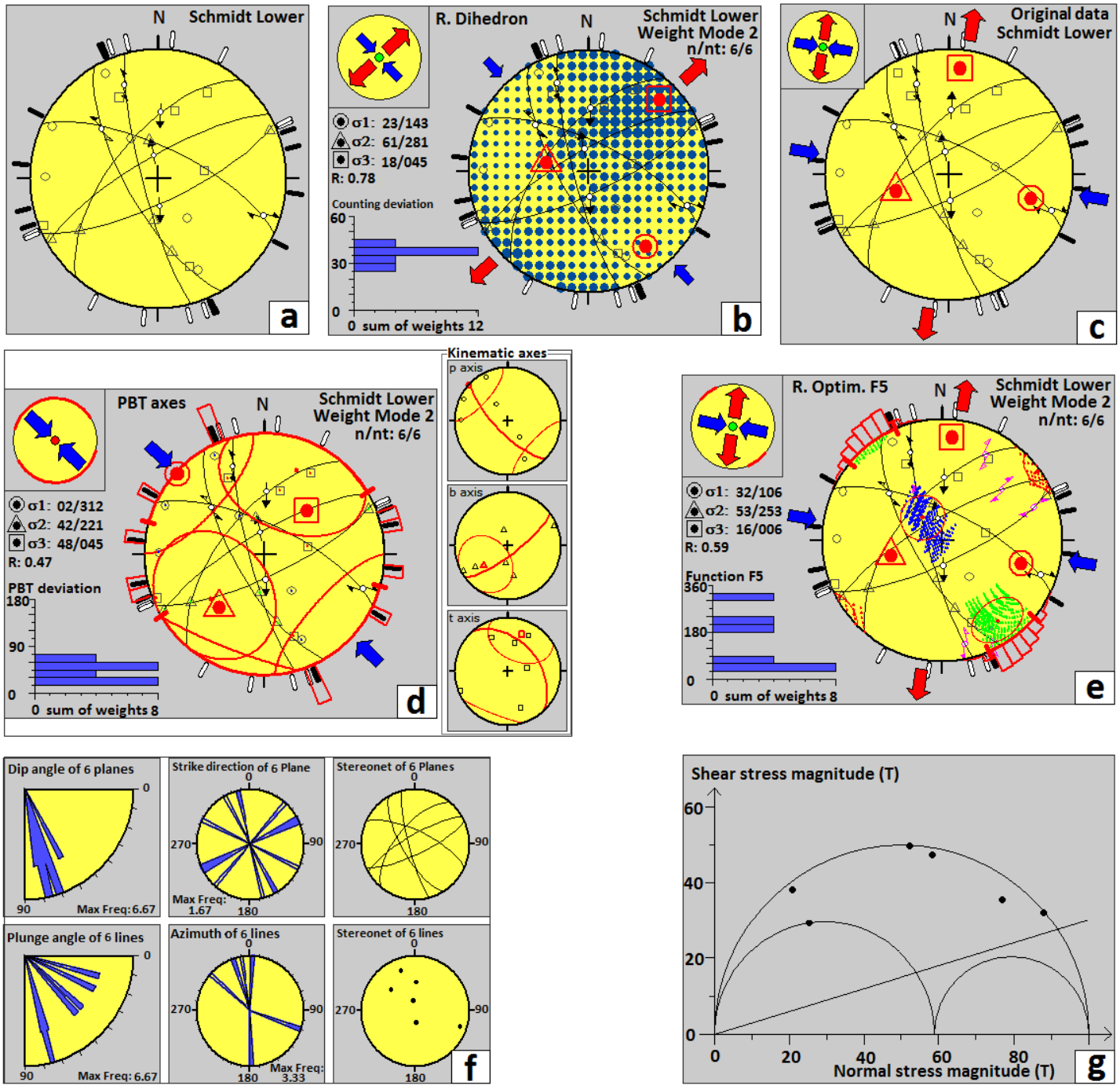

Figure 5: Stress determination for Cretaceous rocks located in eastern part of study area using: **a**) Stereoplot of faults, **b**) Right Dihedron method, **c**) Original data, d) PBT axes method, **e**) Rotational Optimization method, **f**) Rose diagram and stereonet of planes and lines, **g**) Mohr circle.

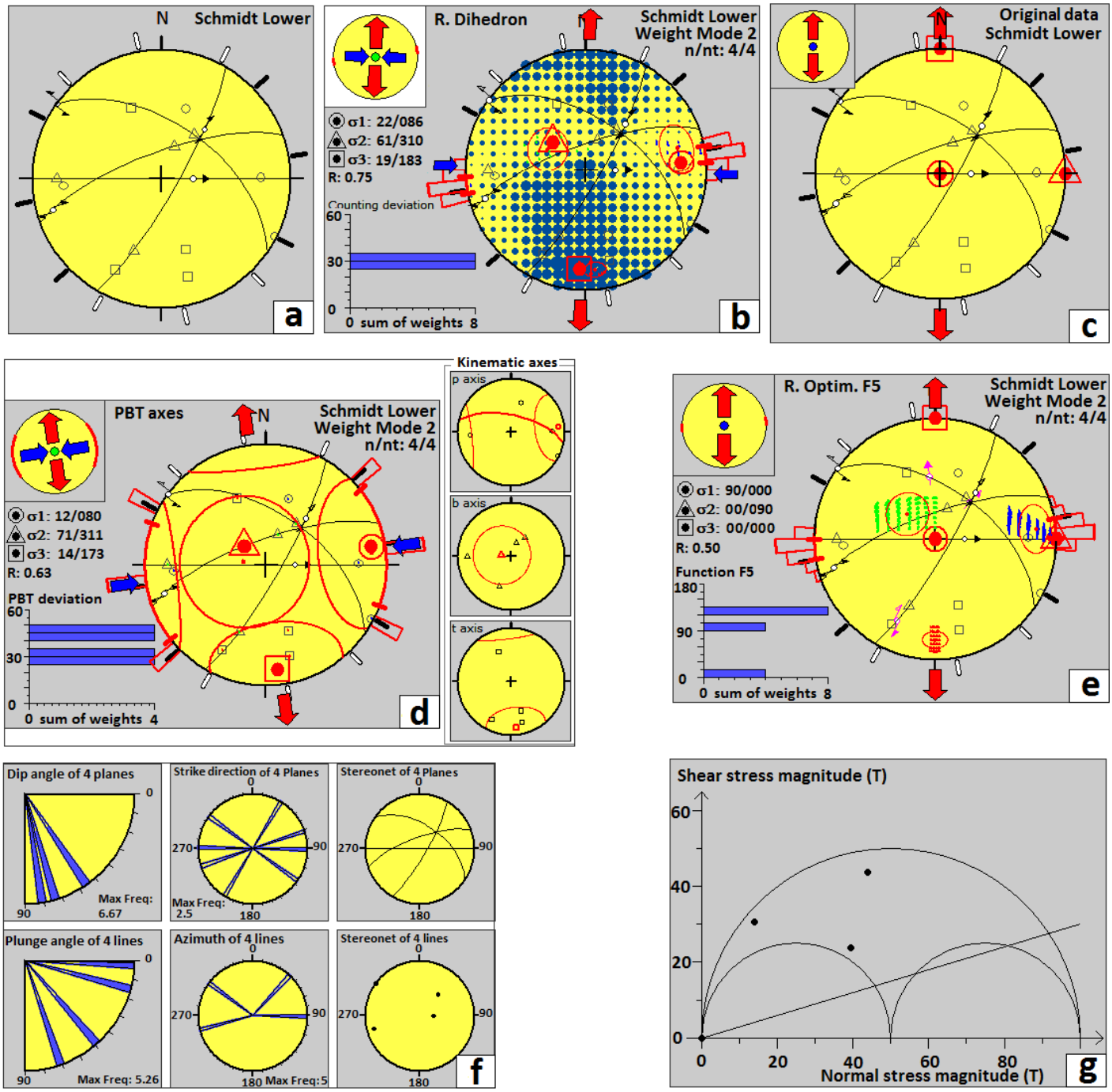

Figure 6: Stress determination for Paleocene rocks located in eastern part of study area using: **a**) Stereoplot of faults, **b**) Right Dihedron method, **c**) Original data, **d**) PBT axes method, **e**) Rotational Optimization method, **f**) Rose diagram and stereonet of planes and lines, **g**) Mohr circle.

In the sections of the Shekarab Mountains we observed the uplift of igneous units the Φ ratio is close to 0.5, stress regime is purely extensional and the shape of stress ellipsoid has been displaced locally from the prolate to the oblate which is due to local change in stress regime (Table **1**). In areas where we observe the uplift of igneous masses, the shape of stress ellipsoid has been displaced locally from the prelate to the oblate, which is due to a local change in stress in these areas. Moreover, in the part of mountain ranges, which has a higher uplift the shape of stress ellipsoid is also oblate. To find out the reason of more outcropping andesitic and dacitic units in eastern section of the Shekarab Mountains, fault data's adjacent to andesitic and dacitic units separated from

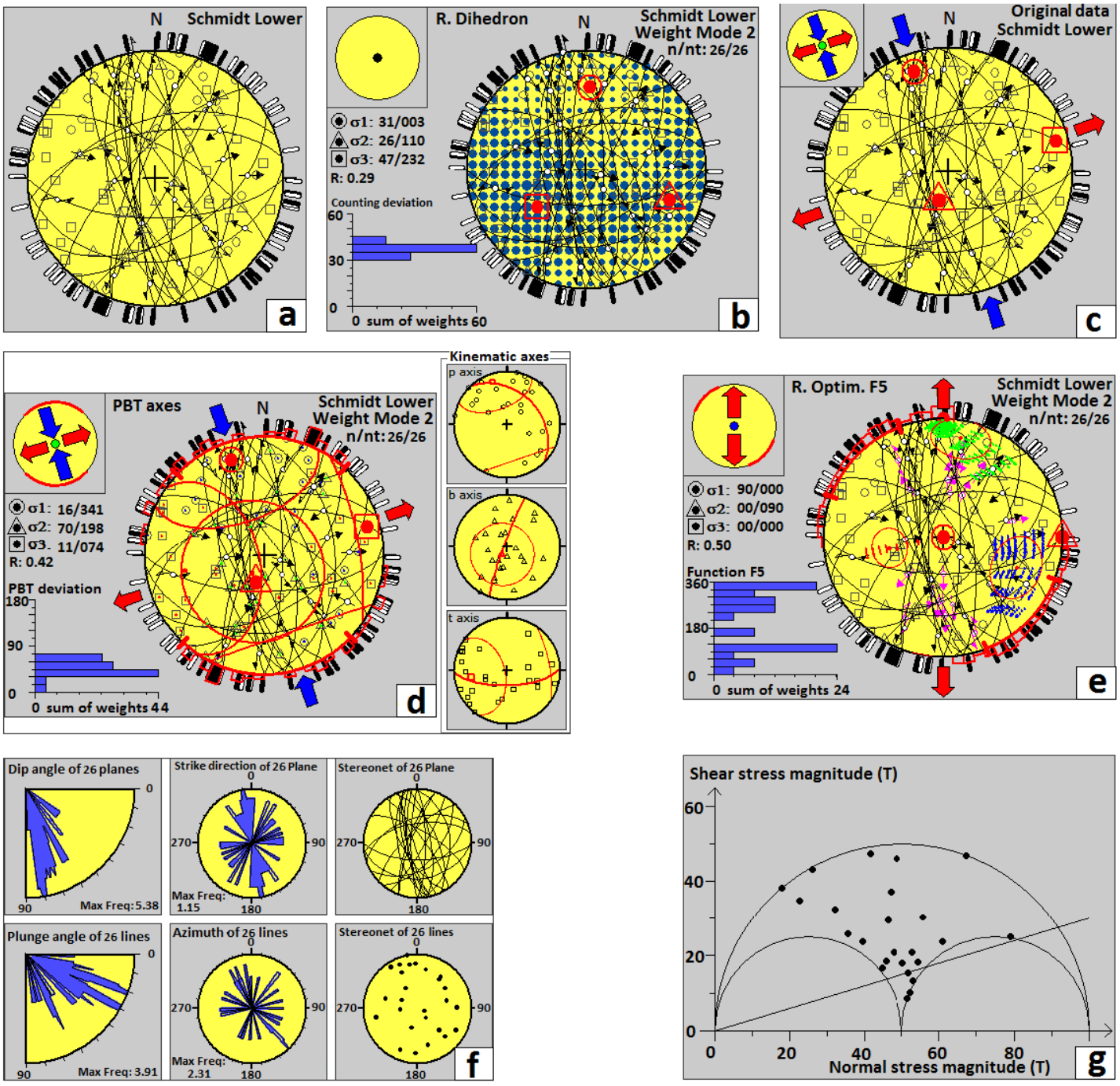

Figure 7: Stress determination for Eocene rocks located in eastern part of study area using: **a**) Stereoplot of faults, **b**) Right Dihedron method, **c**) Original data, **d**) PBT axes method, **e**) Rotational Optimization method, **f**) Rose diagram and stereonet of planes and lines, **g**) Mohr circle.

other Eocene's faults related to the eastern part of the Shekarab Mountains and were interpreted using Right Dihedron, PBT axes and Rotational Optimization methods. The faults component adjacent to the igneous units are normal with strike-slip components; analysis of relationships between stress regime changes and exhumation indicate that in the areas we observe the exhumation of igneous units the shape of stress ellipsoid has been changed locally from prolate to oblate which is due to local change of stress regime, The transtensive stress regime of the adjacent faults of igneous units has caused exhumation and outcrop of Eocene igneous units in the eastern part of the Shekarab Mountains, and minor stress axis (σ3) direction has been displaced locally to East-West trend. Local variation of stress regime in the eastern part of Shekarab Mountains caused the boarder outcrops of igneous units (Table **1**, Fig. **15**).

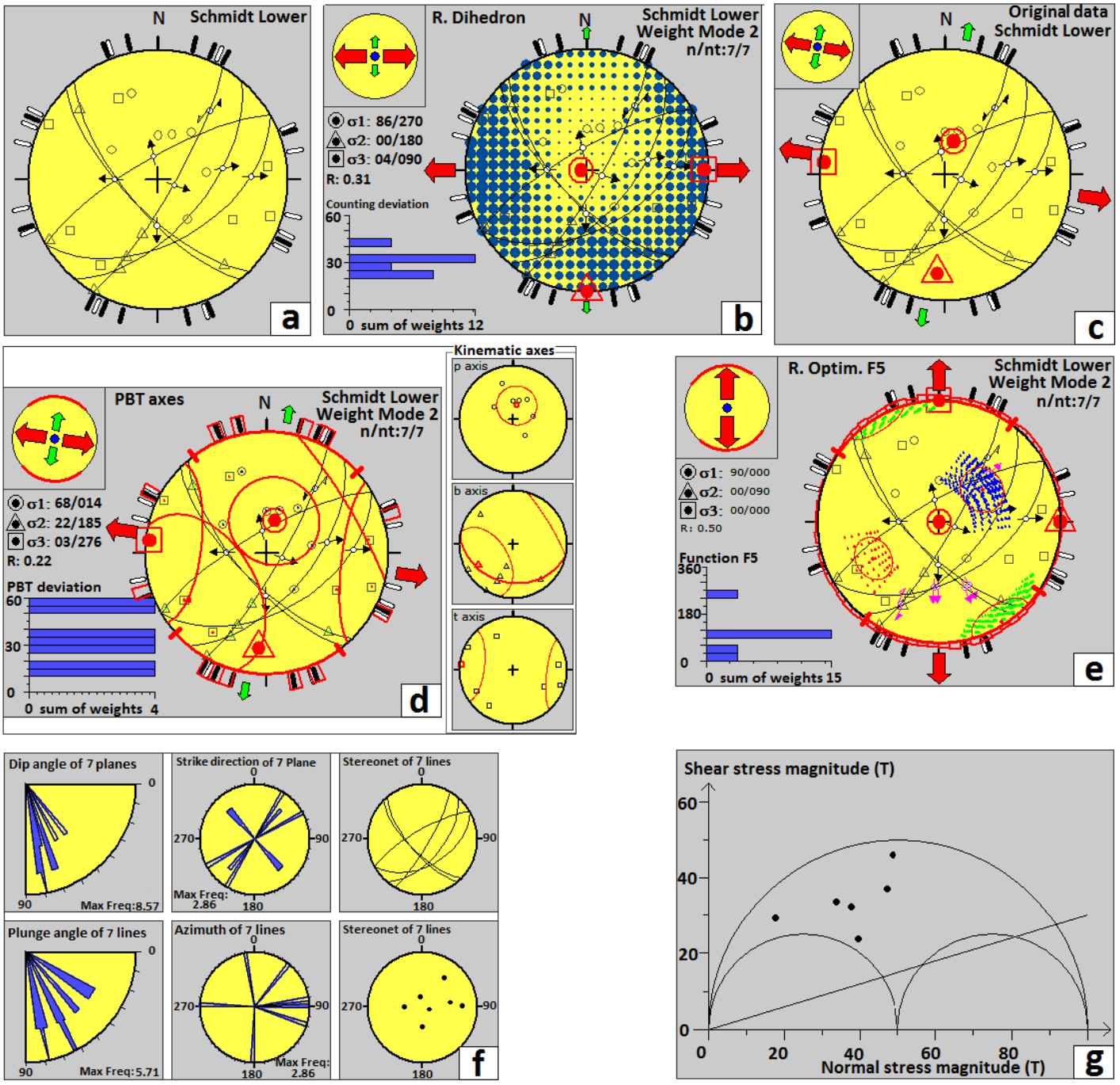

Figure 8: Stress determination for Eocene rocks located in middle part of study area using: **a**) Stereoplot of faults, **b**) Right Dihedron method, **c**) Original data, **d**) PBT axes method, **e**) Rotational Optimization method, **f**) Rose diagram and stereonet of planes and lines, **g**) Mohr circle.

Table 1: Stress tensors for different geological time rock unites in the studied area.

Rock Units	σ1	σ2	σ3	Φ
East Crt	312/02	221/42	045/48	0.78
East paleocene	086/22	310/61	183/19	0.75
East Eocene	003/31	110/26	232/47	0.29
East oligocene	359/38	189/52	093/05	0.52

Table 1 (contd....)

Rock Units	σ1	σ2	σ3	Φ
East miocene	114/01	204/28	021/62	0.5
East volcanic mass	270/86	180/00	090/04	0.31
middle Eocene	345/20	100/50	242/33	0.6
middle oligocene	355/44	164/45	259/06	0.48
Middle Quternary	060/10	277/77	152/08	0.5
west Eocene	187/08	095/11	311/77	0.64

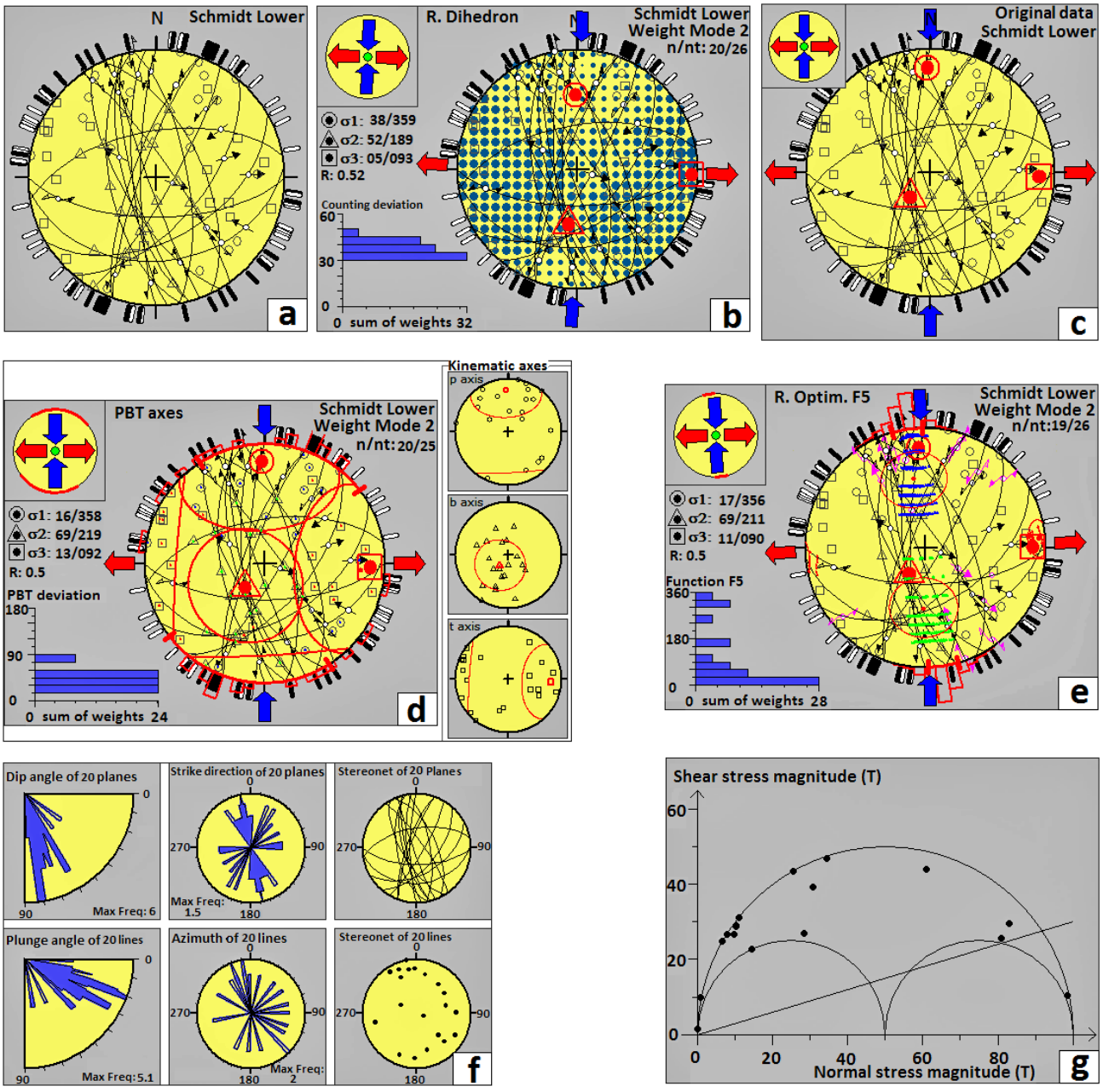

Figure 9: Stress determination for Eocene rocks located in western part of study area using: **a**) Stereoplot of faults, **b**) Right Dihedron method, **c**) Original data, **d**) PBT axes method, **e**) Rotational Optimization method, **f**) Rose diagram and stereonet of planes and lines, **g**) Mohr circle.

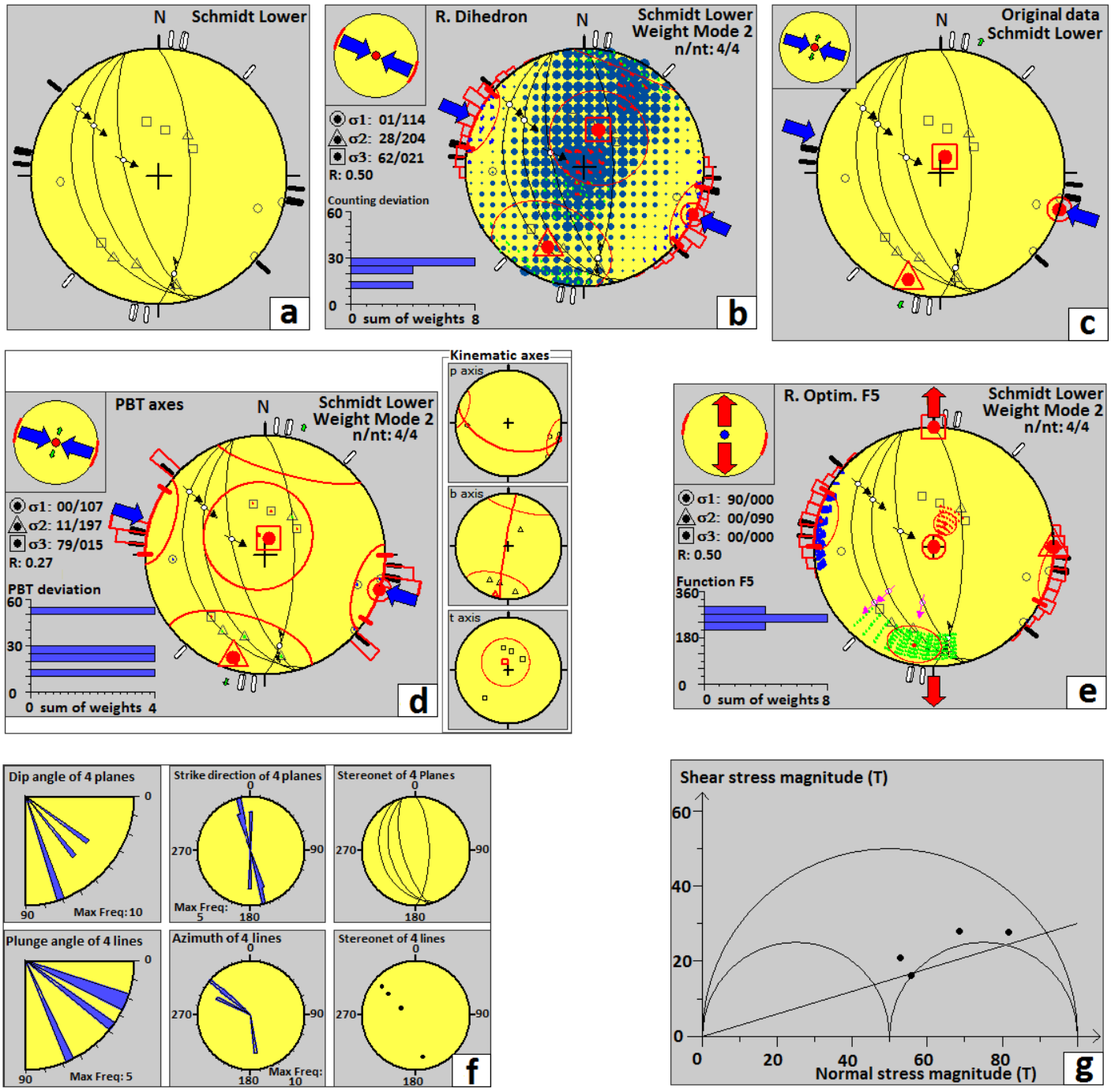

Figure 10: Stress determination for Andsite and Dacite units of Eocene located in eastern part of study area using: **a**) Stereoplot of faults, **b**) Right Dihedron method, **c**) Original data, **d**) PBT axes method, **e**) Rotational Optimization method, **f**) Rose diagram and stereonet of planes and lines, **g**) Mohr circle.

Structural analysis and analysis of Steps of applied Paleo stress in Shekarab Mountains indicate that in Cretaceous time stress regime operation tectonic was strike-slip. Most outcrops of igneous units (andesite and dacite) by the age of Eocene is related to the eastern part of the Shekarab Mountains, in the sections of the Shekarab Mountains we observed the uplift of igneous units the shape of stress ellipsoid has been displaced locally from the prolate to the oblate which is due to local change in stress in this areas. Results of this research indicate that major stress axis (σ1) in Cretaceous units show NW-SE trend, in Eocene units show approximately N-S trend and in Quaternary units show NE-SW trend. Accordingly, major stress axis (σ1) in the Shekarab Mountains had clockwise rotation (Fig. **16**). Similar interpretations of stress fields were suggested for the Brittle tectonic

reconstruction of palae-extension inherited from Mesozoic rifting in West Zagros (Kermanshah, Iran) results of this research show that this extension characterizes a stretched continental margin similar to the present-day passive margin of the British Isles. Considering the structural pattern of the inherited basement faults, as revealed by the present-day earthquake focal mechanisms, an oblique crustal stretching model is proposed for the rifting process [49]; brittle deformation and states of paleostress constrained by fault kinematics in the central German platform results of this research indicate that fracture patterns of both the cover and basement rocks appear to record the same states of stress [50]; Plio-Quaternary kinematic development and paleostress pattern of the Edremit Basin [51], western Turkey results of this research show that the North Anatolian Fault System is the prominent structure in the current morphotectonic framework of the Edremit Gulf and adjacent areas [33].

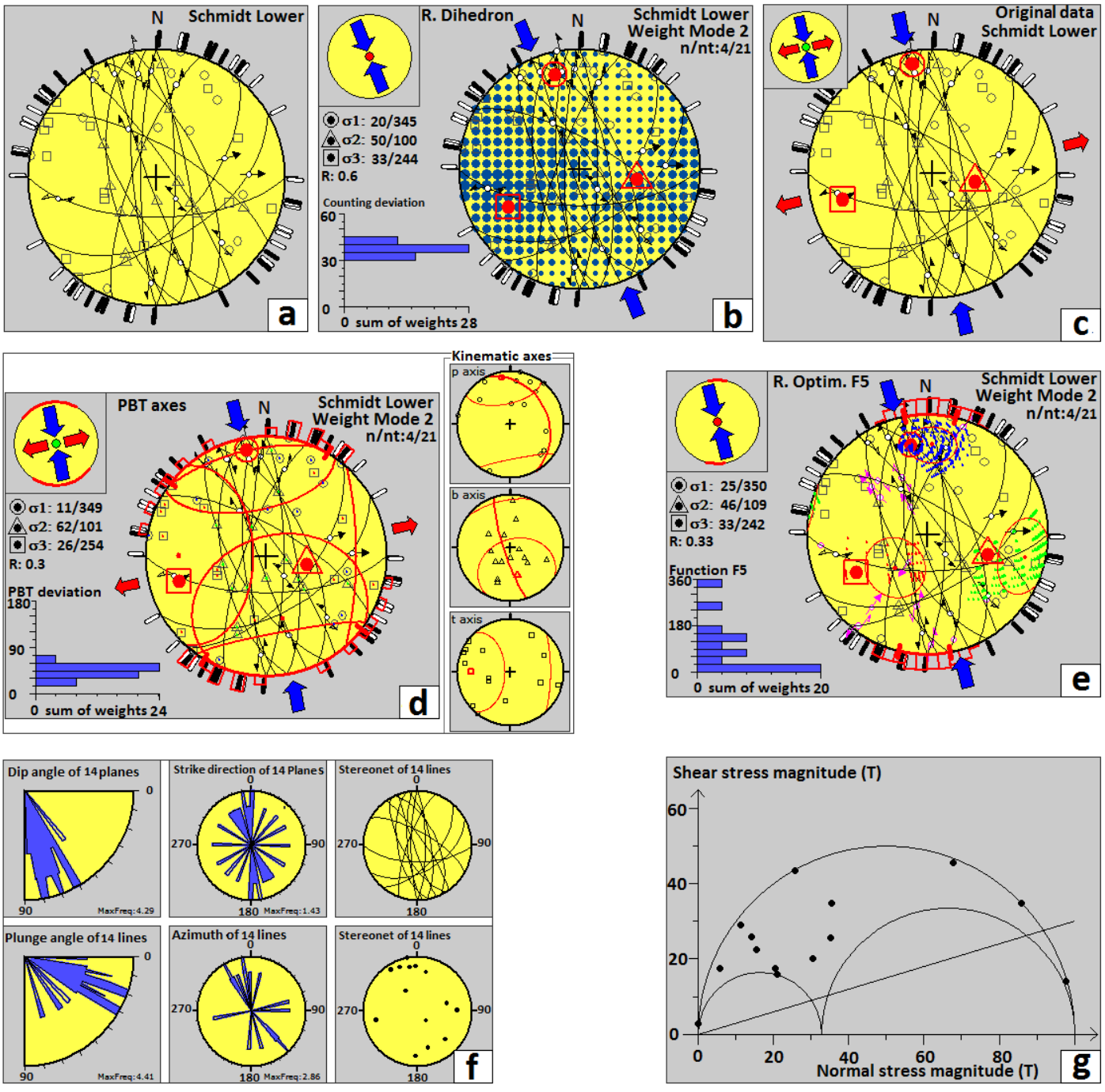

Figure 11: Stress determination for Oligocene rocks located in eastern part of study area using: **a**) Stereoplot of faults, **b**) Right Dihedron method, **c**) Original data, **d**) PBT axes method, **e**) Rotational Optimization method, **f**) Rose diagram and stereonet of planes and lines, **g**) Mohr circle.

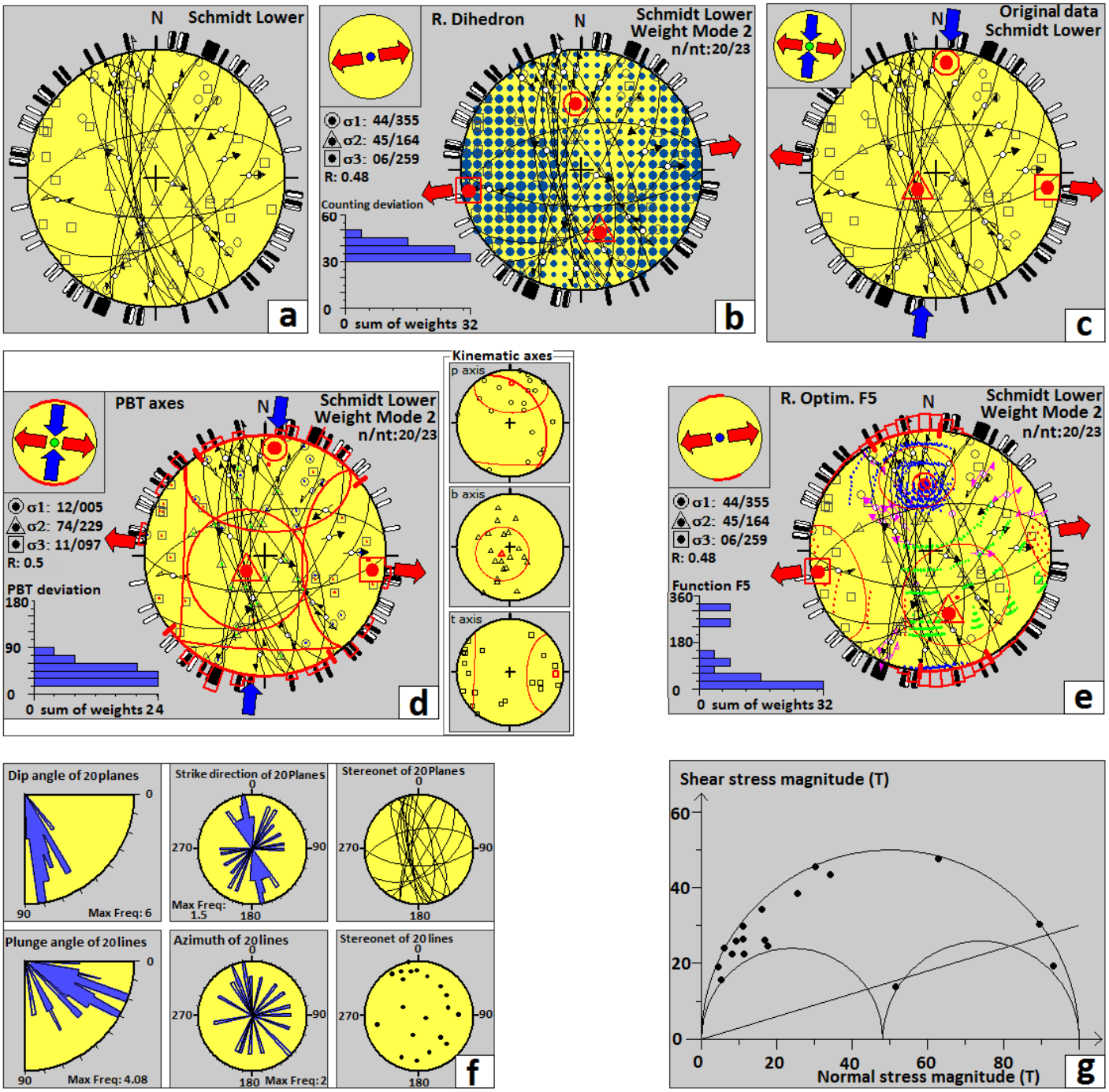

Figure 12: Stress determination for Oligocene rocks located in middle part of study area using: **a**) Stereoplot of faults, **b**) Right Dihedron method, **c**) Original data, **d**) PBT axes method, **e**) Rotational Optimization method, **f**) Rose diagram and stereonet of planes and lines, **g**) Mohr circle.

5. Conclusion

Inversion of the separated data sets allows us to distinguish that there are episodic changes in stress regimes in the Shekarab Mountains. The separation of fault kinematics data in study area reveals the existence of three successive and continuous stress regimes. The Quaternary stress state, deduced from fault kinematics analysis using conglomerates, indicate that direction of compression (σ1) is close to N026˚. The compression direction in north Sistan suture zone on the basis of inversion of earthquake focal mechanisms is close to N25˚E, this

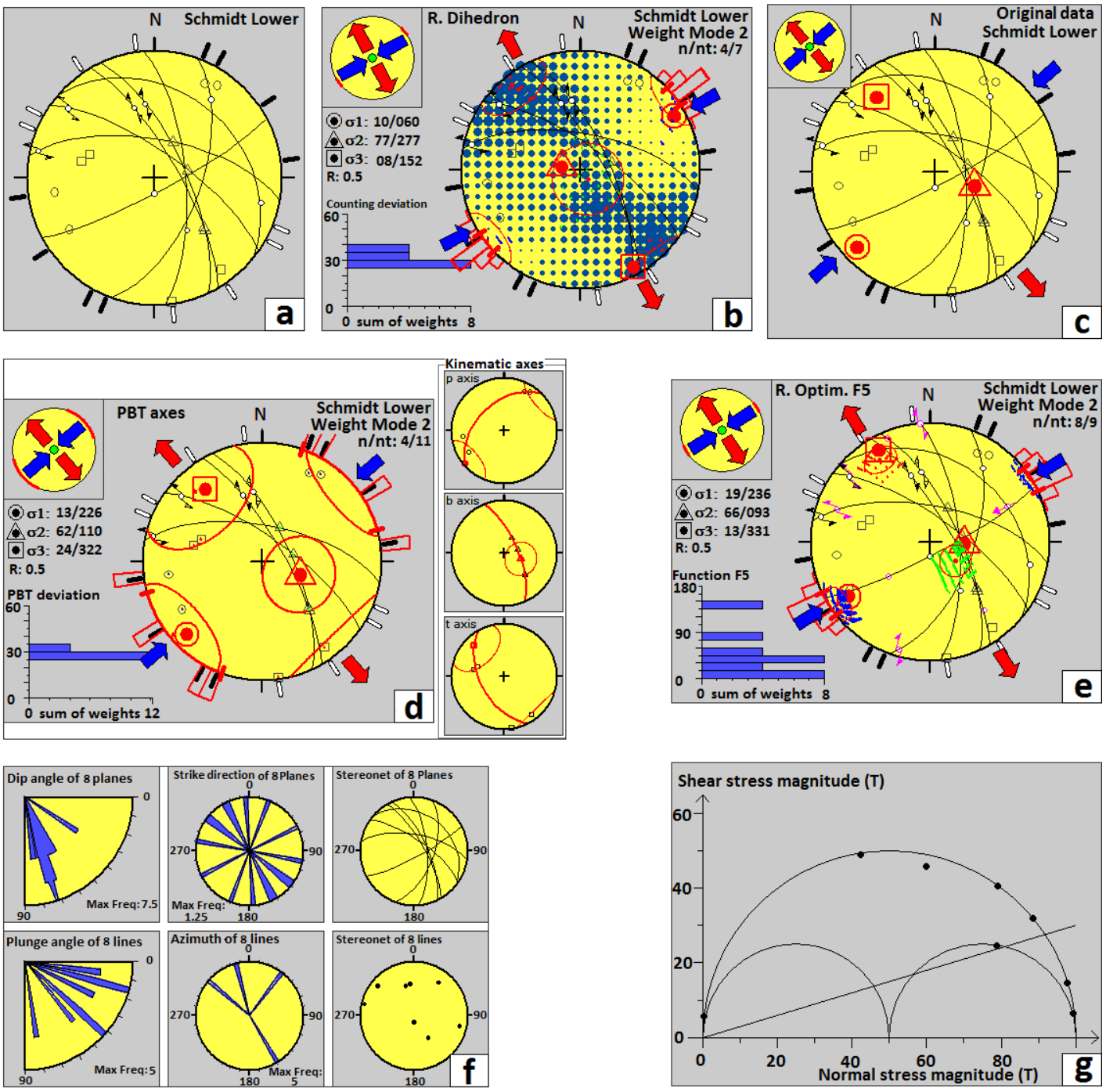

Figure 13: Stress determination for Miocene rocks located in eastern part of study area using: **a**) Stereoplot of faults, **b**) Right Dihedron method, **c**) Original data, **d**) PBT axes method, **e**) Rotational Optimization method, **f**) Rose diagram and stereonet of planes and lines, **g**) Mohr circle.

compression direction is consistent with the mean trend of compressional P axes of earthquakes focal mechanisms. Our stress analyses of brittle structures in Shekarab Mountains reveals drastic changes in stress tensors from Cretaceous to Quaternary ages. Results of our research indicate that direction of compression (σ1) was from N337˚ during the Cretaceous-Paleocene to N003˚ during the Eocene and N026˚ during Oligocene to Quaternary; therefore, direction of compression (σ1) had clockwise rotation at least 49˚ over the last 83 Myr. Our compilation of paleostress data indicates that there have been different distinct stress regimes in study area: 1) compression in the Cretaceous time, 2) transpresion from Paleocene to Miocene times, 3) transtension in the time Oligocene and 4) shear in the Quaternary time. Results of this research indicate that evolution of stress regime

was corresponding to various tectonic events in the Shekarab Mountains. The state of stresses in upper Eocene to Oligocene shows two distinct transpresional and transtensional tectonic regimes. The changes from transpresion to transtension in eastern Shekarab Mountains are due to local variation of stress regime in the sites 9 and 16. The data collected from the sites 9 and 16 are obviously different from the state of stress in Oligocene age; regional changes of stress regime from transpresional to transtensional in the eastern part of study area led to outcropping of igneous rocks (andesite and dacite). The first step of applied stress in the Shekarab Mountains was compressional with the direction of the main stress axes σ1=337/26, σ2=070/06, σ3=172/64, and Φ ratio was 0.1 which caused the uplifting of peridotites and ophiolites in eastern part of study area. The second step of stress has been transpressive with the direction of the main stress axes σ1=003/31, σ2=110/26, σ3=232/47, and Φ ratio was 0.29. The third step of stress regime in Shekarab Mountains is shear with the direction of the main stress axes σ1=026/10, σ2=193/72, σ3=119/08, and Φ ratio 0.5.

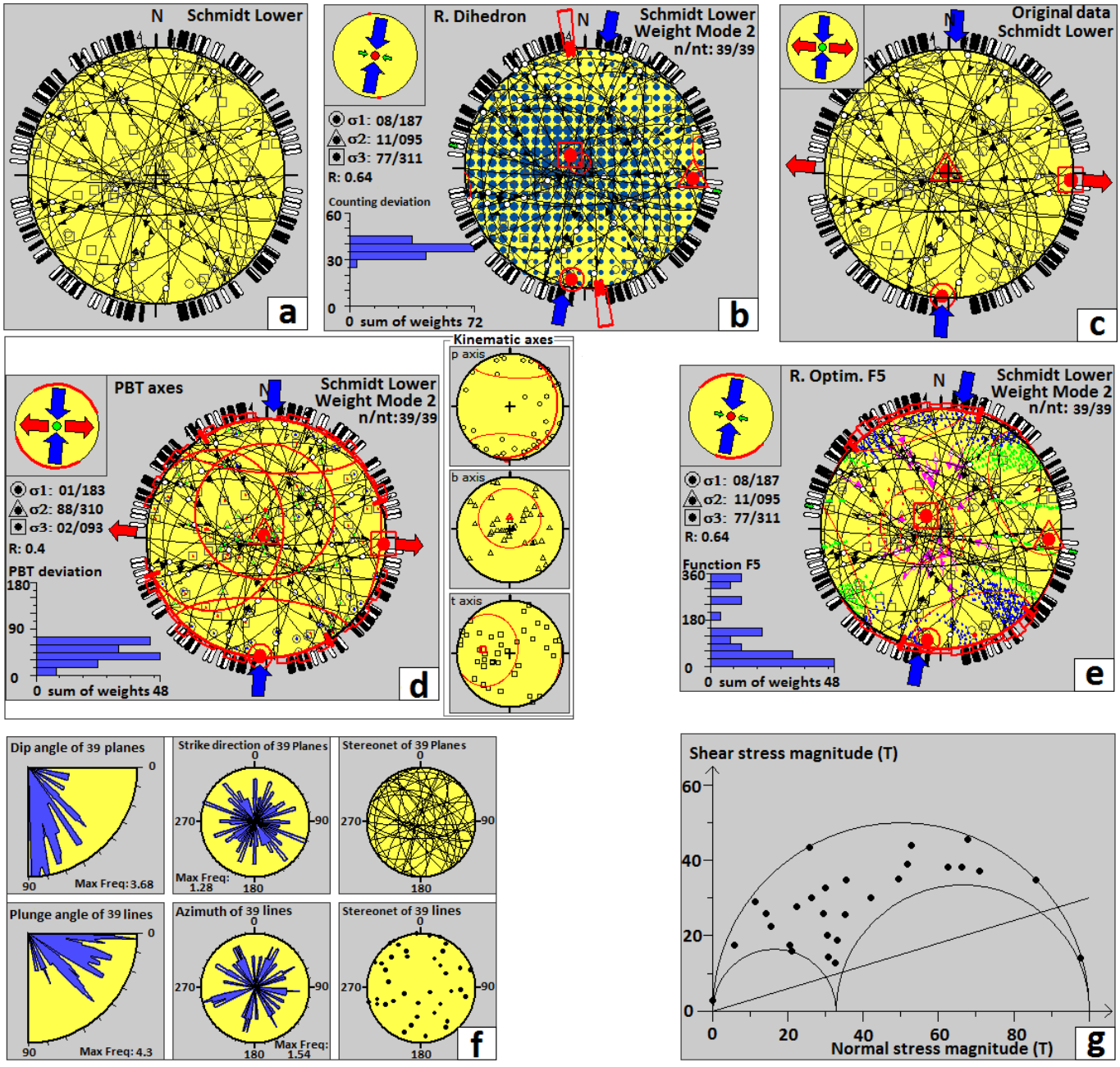

Figure 14: Stress determination for Quaternary rocks located in middle part of study area using: **a**) Stereoplot of faults, **b**) Right Dihedron method, **c**) Original data, **d**) PBT axes method, **e**) Rotational Optimization method, **f**) Rose diagram and stereonet of planes and lines, **g**) Mohr circle.

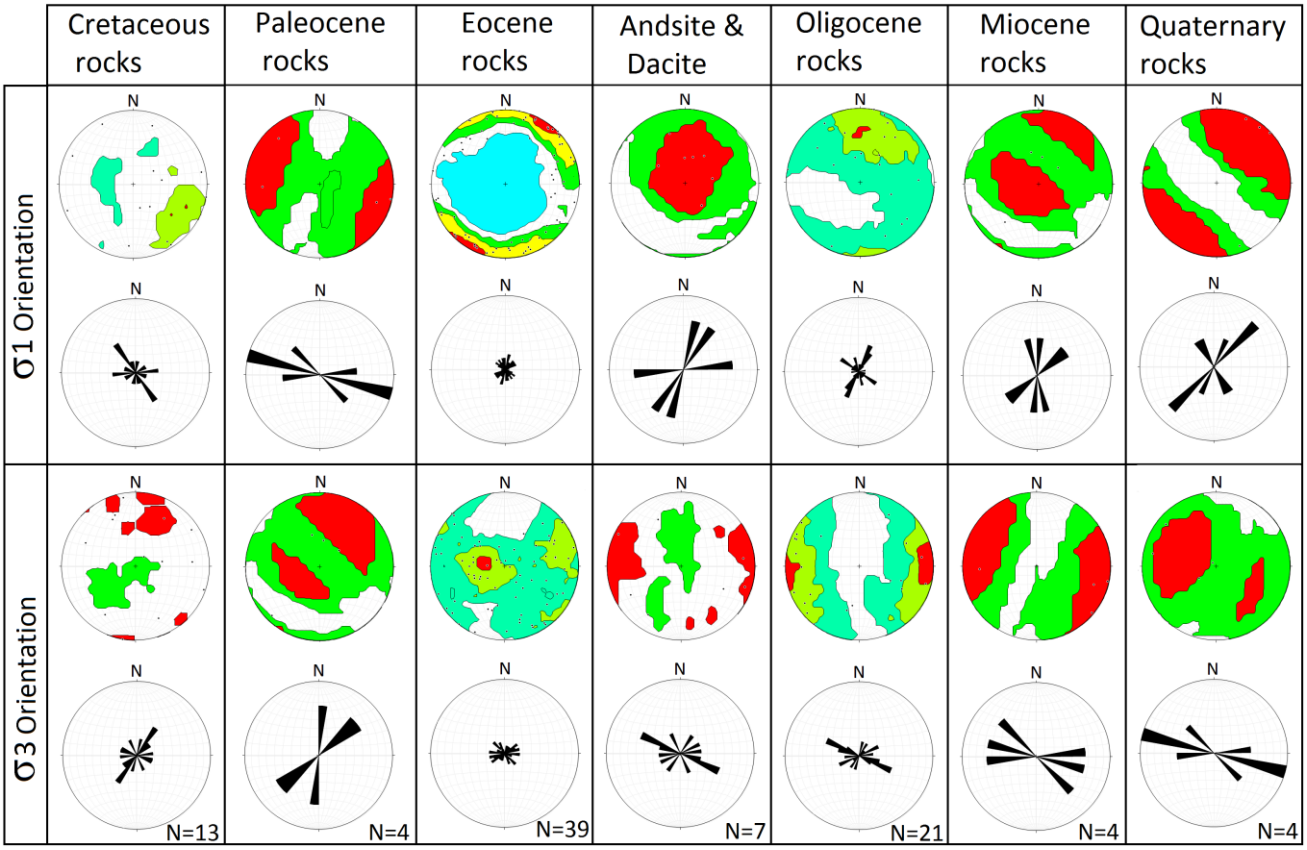

Figure 15: Density stereoplots for σ1 and σ3 orientations and rose diagram for σ1 and σ3 for the tow paleostress fields obtained, 1 ˚⁄₀ contour intervals represented in lower-hemisphere, equal-area projection.

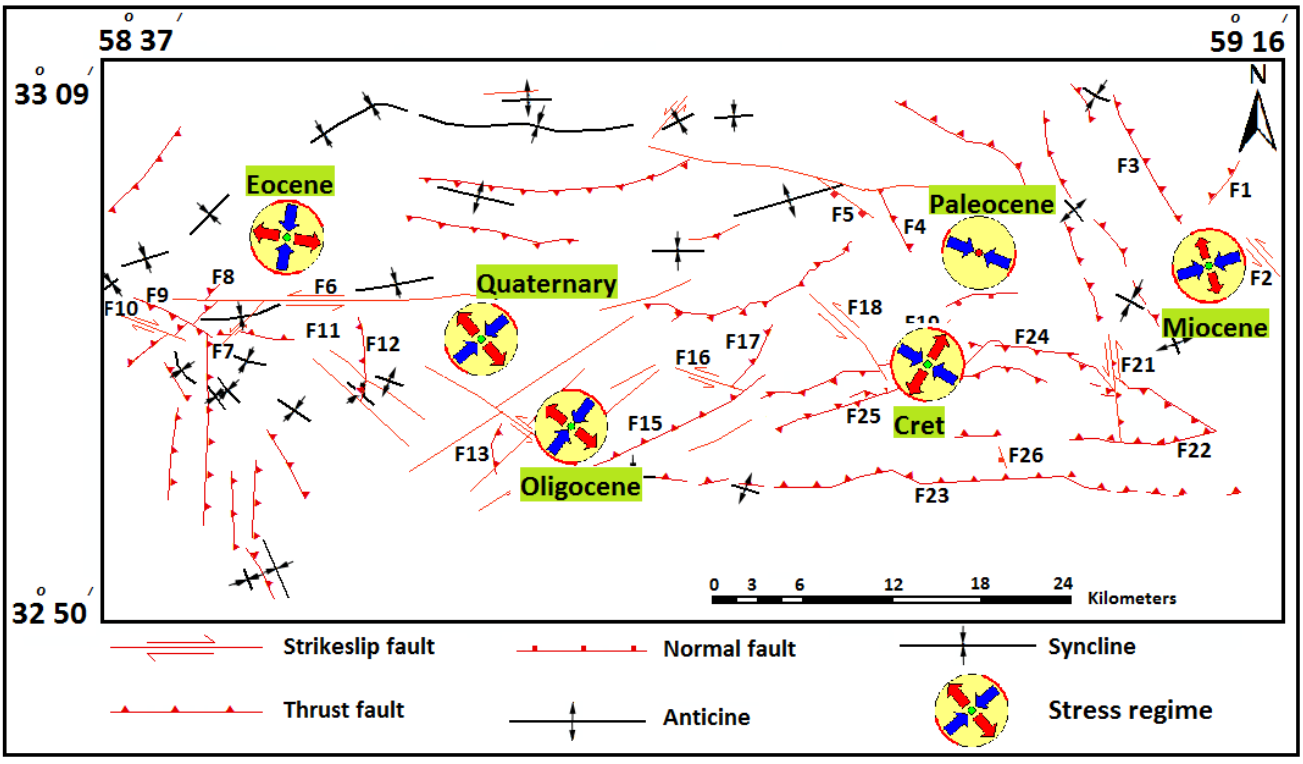

Figure 16: Stress regime map of study area based on fault analysis.

Conflict of Interest

The authors declare no conflict of interest.

Funding

The authors declare that no fund received for this manuscript.

Acknowledgements

The authors thank the University of Birjand for supporting this research.

References

[1] Jackson J, Mc Kenzie D. Active tectonics of the Alpine-Himalayan Belt between Turkey and Pakistan. Geophys J Royal Astronom Soc. 1984; 77: 185-264. https://doi.org/10.1111/j.1365-246X.1984.tb01931.x

[2] Vernant P, Nilforoushan F, Hatzfeld D, Abbassi MR, Vigny C, Masson F, et al. Presentday crustal deformation and plate kinematics in the Middle East constrained by GPS measurements in Iran and northern Oman. Geophys J Int. 2004; 157: 381-98. http://dx.doi.org/10.1111/j.1365-246X.2004.02222.x

[3] Hollingsworth J. Active tectonics of NE Iran. Ph.D Thesis, University of Cambridge; 2007.

[4] Ezati M, Gholami E. Neotectonics of the Central Kopeh Dagh drainage basins, NE Iran. Arab J Geosci. 2022; 15: 995.

[5] Tirrul R, Bell IR, Griffis RJ, Camp VE. The Sistan suture zone of eastern Iran. Geol Soc Am Bull. 1983; 94: 134-50. https://doi.org/10.1130/0016-7606(1983)94<134:TSSZOE>2.0.CO;2

[6] Hu W, Zheng Y, McSaveney M, Xu Q, Huang R, Zhou L. Evolution of the strain localization and shear-zone internal structure in the granular material: Insights from ring-shear experiments. Eng Geol. 2023; 325: 107283. https://doi.org/10.1016/j.enggeo.2023.107283

[7] Molnar P, Tapponnier P. Cenozoic tectonics of Asia: effect collision of a continental. Science. 1975; 189: 419-26.

[8] Lin Y, Zong Z, Bi K, Hao H, Lin J, Chen Y. Experimental and numerical studies of the seismic behavior of a steel-concrete composite rigid-frame bridge subjected to the surface rupture at a thrust fault. Eng Struct. 2020; 205: 110105. https://doi.org/10.1016/j.engstruct.2019.110105

[9] Parlangeau C, Lacombe O, Schueller S, Daniel JM. Inversion of calcite twin data for paleostress orientations and magnitudes: A new technique tested and calibrated on numerically-generated and natural data. Tectonophysics, 2017; 722: 462-85. https://doi.org/10.1016/j.tecto.2017.09.023

[10] Li Q, Song D, Yuan C, Nie W. An image recognition method for the deformation area of open-pit rock slopes under variable rainfall. Measurement. 2022; 188: 110544. https://doi.org/10.1016/j.measurement.2021.110544

[11] Li X, Li Q, Wang Y, Liu W, Hou D, Zheng W, et al. Experimental study on instability mechanism and critical intensity of rainfall of high-steep rock slopes under unsaturated conditions. Int J Min Sci Technol. 2023; 33(10): 1243-60. https://doi.org/10.1016/j.ijmst.2023.07.009

[12] Mameri L, Tommasi A, Vauchez A, Signorelli J, Hassani R. Structural inheritance controlled by olivine viscous anisotropy in fossil mantle shear zones with different past kinematics. Tectonophysics. 2023; 863: 229982. https://doi.org/10.1016/j.tecto.2023.229982

[13] Angelier J. Inversion of earthquake focal mechanisms to obtain the seismotectonic stress IV—a new method free of choice among nodal planes. Geophys J Int. 2002; 150: 588-609. https://doi.org/10.1046/j.1365-246X.2002.01713.x

[14] Sasvári Á, Baharev A. SG2PS (structural geology to postscript converter) – A graphical solution for brittle structural data evaluation and paleostress calculation. Comput Geosci. 2014; 66: 81-93. https://doi.org/10.1016/j.cageo.2013.12.010

[15] Mercier J, Carey-Gailhardis LE, Sebrier M, Stein S, Mercier JL, Hancock P. Palaeostress determinations from fault kinematics: Application to the neotectonics of the Himalayas-Tibet and the Central Andes [and discussion], Philos Trans R Soc A. 1991; 337: 41-52. https://doi.org/10.1098/rsta.1991.0105

[16] Rowan MG, Muñoz JA, Roca E, Ferrer O, Santolaria P, Granado P, et al. Linked detachment folds, thrust faults, and salt diapirs: observations and analog models. J Struct Geol. 2022; 155: 104509. https://doi.org/10.1016/j.jsg.2022.104509

[17] Jackson J. Partitioning of strike-slip and convergent motion between Eurasia and Arabia in eastern Turkey and the Caucasus. J Geophys Res: Solid Earth. 1992; 97(B9): 12471-9. https://doi.org/10.1029/92JB00944

[18] Kaymakci N. Kinematic development and paleostress analysis of the Denizli Basin (Western Turkey): implications of spatial variation of relative paleostress magnitudes and orientations. J Asian Earth Sci. 2006; 27: 207–22. https://doi.org/10.1016/j.jseaes.2005.03.003

[19] Sippel J, Saintot A, Heeremans M, Scheck-Wenderoth M. Paleostress field reconstruction in the Oslo region. Marine Pet Geol. 2009; 27: 682-708. https://doi.org/10.1016/j.marpetgeo.2009.08.010

[20] Bhattacharyya K, Dwivedi HV, Das JP, Damania S. Structural geometry, microstructural and strain analyses of L-tectonites from Paleoproterozoic orthogneiss: Insights into local transport-parallel constrictional strain in the Sikkim Himalayan fold thrust belt. J Asian Earth Sci. 2015; 107: 212-31. https://doi.org/10.1016/j.jseaes.2015.04.038

[21] Ezati M, Agh-Atabi M. Active tectonic analysis of Atrak river subbasin located in NE Iran (East Alborz). J Tethys. 2013; 1: 177-88.

[22] Ezati M, Agh-Atabi M. Estimating rate of tectonic activity in central Kopeh dagh using morphometric indices. J Tethys. 2014: 4: 314-26.

[23] Coubal M, Málek J, Adamovic J, Stepancíková P. Late Cretaceous and Cenozoic dynamics inferred of the Bohemian Massif from the paleostress history of the Lusatian Fault Belt. J Geodyn. 2015; 87: 26-49. http://dx.doi.org/10.1016/j.jog.2015.02.006

[24] Heuberger S, Célérier B, Burg JP, Chaudhry NM, Dawood H, Hussain S. Paleostress regimes from brittle structures of the Karakoram–Kohistan Suture Zone and surrounding areas of NW Pakistan. J Asian Earth Sci. 2010; 38: 307-35. https://doi.org/10.1016/j.jseaes.2010.01.004

[25] Tripathy V, Saha D. Inversion of calcite twin data, Paleostress reconstruction and multiphase weak deformation in cratonic interior-Evidence from the protrozoic Caddapah basin, India. J Struct. Geol. 2015; 77, 62-81. https://doi.org/10.1016/j.jsg.2015.05.009

[26] Shi G, Shen C, Zattin M, Wang H, Yang C, Liang C. Late Cretaceous-Cenozoic exhumation of the Helanshan Mt Range, western Ordos fold-thrust belt, China: Insights from structural and apatite fission track analyses. J Asian Earth Sci. 2019; 176: 196-208. https://doi.org/10.1016/j.jseaes.2019.02.016

[27] Arai N, Chigira M. Distribution of gravitational slope deformation and deep-seated landslides controlled by thrust faults in the Shimanto accretionary complex. Engineering Geology, 2019; 260: 105236. https://doi.org/10.1016/j.enggeo.2019.105236

[28] Bose S, Das A, Samantaray S, Banerjee S, Gupta S. Late tectonic reorientation of lineaments and fabrics in the northern Eastern Ghats Province, India: Evaluating the role of the Mahanadi Shear Zone. J Asian Earth Sci. 2020; 201: 104071. https://doi.org/10.1016/j.jseaes.2019.104071

[29] Ezati M, Gholami E, Mousavi SM, Rashidi A, Derakhshani R. Active Deformation Patterns in the Northern Birjand Mountains of the Sistan Suture Zone, Iran. Appl Sci. 2022a; 12: 6625. https://doi.org/10.3390/app12136625

[30] Ezati M, Gholami E, Mousavi SM, Rashidi A, Ezati, M. Structural style and kinematic analysis of the northern Birjand Mountain range, Sistan suture zone, Eastern Iran. Arab J Geosci. 2023; 16: 389. https://doi.org/10.1007/s12517-023-11504-z

[31] Ezati M, Gholami E, Mousavi SM. Paleostress regime reconstruction based on brittle structures analysis in the Shekarab Mountain, Eastern Iran. Arab J Geosci. 2020; 13: 1232. https://doi.org/10.1007/s12517-020-06235-4

[32] Ezati M, Gholami E, Mousavi SM. Tectonic activity level evaluation using geomorphic indices in the Shekarab Mountains, Eastern Iran. Arab J Geosci. 2021; 14: 385. https://doi.org/10.1007/s12517-021-06724-0

[33] Ezati M, Rashidi A, Gholami E, Mousavi SM, Nemati M, Shafieibafti S, et al. Paleostress Analysis in the Northern Birjand, East of Iran: Insights from Inversion of Fault-Slip Data, minerals 2022b; 12: 1606. https://doi.org/10.3390/min12121606

[34] Smeraglia L, Fabbi S, Maffucci R, Albanesi L, Carminati E, Billi A, et al. The role of post-orogenic normal faulting in hydrocarbon migration in fold-and-thrust belts: Insights from the central Apennines, Italy. Marine Pet Geol. 2022; 136: 105429. https://doi.org/10.1016/j.marpetgeo.2021.105429

[35] Elitez İ, Yaltırak, C. Miocene to Quaternary geodynamic evolution of the southern section of the Burdur-Fethiye Shear Zone and its offshore continuation, eastern Mediterranean. Tectonophysics. 2023; 857: 229866. https://doi.org/10.1016/j.tecto.2023.229866

[36] Li Y, Xu WL, Zhang XM, Tang J. Petrogenesis of Jurassic granitic plutons in the Yanbian area NE China: Implications for the subduction history of the Paleo-Pacific Plate. J Asian Earth Sci. 2023; 259: 105940. https://doi.org/10.1016/j.jseaes.2023.105940

[37] Martin AK. Opposite rotations in the Central Andes Bend: Tectonic scenario compared to other cases of opposite rotations and implications for long-term subduction at continental arcs. J South Am Earth Sci. 2023; 104698. https://doi.org/10.1016/j.jsames.2023.104698

[38] McFadden RR, Taylor JM, Whitney DL, Teyssier C, Seaton NCA, Schroeder H. Deformation conditions and kinematic vorticity within the footwall shear zone of the Wildhorse detachment system, Pioneer metamorphic core complex, Idaho. J Struct Geol. 2023; 105031. https://doi.org/10.1016/j.jsg.2023.105031

[39] Rashidi A, Shafieibafti Sh, Nemati M, Ezati M, Gholami E, Mousavi SM. Flexural-slip folding in buckling phases of orogenic belts: insight into the tectonic evolution of fault splays in the East Iran Orogen. Front Earth Sci. 2023; 11: 531. https://doi.org/10.3389/feart.2023.1169667

[40] Simonetti M, Langone A, Bonazzi M, Corvò S, Maino M. Tectono-metamorphic evolution of a post-variscan mid-crustal shear zone in relation to the Tethyan rifting (Ivrea-Verbano Zone, Southern Alps). J Struct Geol. 2023; 173: 104896. https://doi.org/10.1016/j.jsg.2023.104896

[41] Su J. Accelerated subduction of the western Pacific Plate promotes the intracontinental uplift and magmatism in late Jurassic South China. Tectonophysics. 2023; 230136. https://doi.org/10.1016/j.tecto.2023.230136

[42] Camp VE, Griffis, RJ. Character, genesis and tectonic setting of igneous rocks in the Sistan suture zone, eastern Iran. Lithos. 1982; 3: 221-39. https://doi.org/10.1016/0024-4937(82)90014-7

[43] Berberian M, Yeats RS. 1999. Patterns of historical earthquake rupture in the Iranian plateau. Bull Seismol Soc Am. 1999; 89: 120-39. https://doi.org/10.1785/BSSA0890010120

[44] Khatib MM. Structural analysis of southern Birjand Mountains. PhD Thesis. Shahid Beheshti University; Tehran: 1998.

[45] Vahdati Daneshmand F, Kholghi MH. 1/100000 Geological map of Khusf. Geol Surv Tehran Iran, 1986.

[46] Simón JL. Forty years of paleostress analysis: has it attained maturity? J Struct Geol. 2018; 1-35. https://doi.org/10.1016/j.jsg.2018.02.011

[47] Wakabayashi J. Subducted sedimentary serpentinite mélanges: Record of multiple burial–exhumation cycles and subduction erosion. Tectonophysics. 2012; 568: 230-47.

[48] Delvaux D. Win-Tensor, an interactive computer program for fracture analysis and crustal stress reconstruction. Geophys Res Abs. 2011; 13: 4018.

[49] Navabpour P, Angelier J, Barrier E. Brittle tectonic reconstruction of palaeo-extension inherited from Mesozoic rifting in West Zagros (Kermanshah, Iran). J Geol Soc. 2011; 168: 979-94. https://doi.org/10.1144/0016-76492010-108

[50] Navabpour P, Malz A, Kley J, Siegburg M, Kasch N, Ustaszewski K. Intraplate brittle deformation and states of paleostress constrained by fault kinematics in the central German platform. Tectonophysics. 2017; 694: 146-63. https://doi.org/10.1016/j.tecto.2016.11.033

[51] Gürer ÖF, Sangu E, Özburan M, Gürbüz A, Gürer A, Sinir H. Plio-Quaternary kinematic development and paleostress pattern of the Edremit Basin, western Turkey. Tectonophysics. 2016; 679: 199-210. https://doi.org/10.1016/j.tecto.2016.05.007